SPECTROMETRY AND HYPERSPECTRAL REMOTE SENSING FOR ROAD CENTERLINE EXTRACTION AND EVALUATION OF PAVEMENT CONDITION

Val Noronha
Martin Herold
Dar Roberts
Meg Gardner
National Consortium on Remote Sensing in Transportation — Infrastructure Management
Department of Geography
University of California
Santa Barbara CA 93106-4060
noronha@geog.ucsb.edu
martin@geog.ucsb.edu
dar@geog.ucsb.edu
meg@geog.ucsb.edu

ABSTRACT

Remote sensing may offer quick and economical methods of surveying road centerline geometry and condition. This research uses a combination of 4 m, 224-band AVIRIS hyperspectral imagery, and about 6000 field-gathered spectra, to develop a spectral library of urban materials. It attempts to extract roads of various types, and investigates the spectral signatures associated with different qualities of pavement. In general the methods are successful in identifying roads and distinguishing between principal construction materials (e.g. concrete vs asphalt). To a limited extent it has been possible to automate the process of centerline extraction. However, asphalt pavement is spectrally similar to certain types of composite roofing materials, hence classification is imperfect, and considerable additional research is required to perfect the extraction of road signatures. The extraction technique holds promise in rural areas where there is much less potential for confusion between asphalt and surrounding materials. It is possible to estimate *age* of pavement, and to the extent that this correlates with pavement health, hyperspectral analysis is useful, but the traditional indicators of pavement health (e.g. cracking and rutting) are sub-meter phenomena and clearly not detectable in 4 m imagery. Finally, this research argues that since much of the discriminating ability of hyperspectral remote sensing is concentrated within a few wave bands, it should be possible to design a sensor of lower spectral resolution (i.e. multispectral), specifically for transportation and urban remote sensing, that could achieve many of these objectives at a much lower cost.

INTRODUCTION

Geometric centerlines of transportation features are a foundation data set for the management of transportation infrastructure and assets. The quality standards for these data have evolved considerably over the last three decades as applications have become more demanding, with positional accuracy requirements shrinking from tens of meters to a few centimeters. A number of survey technologies have been applied to the centerline problem, ranging from static field survey to GPS and photogrammetry. Each technology has a cost and benefit associated with it, and addresses a niche in the continuum of data quality requirements (Noronha 2001). It would be a simplification to argue that more "accurate" (loosely defined) is necessarily and universally better. Current data models such as UNETRANS (Curtin et al, 2001) link together multiple centerline representations of the same object (e.g. roadway, carriageway and lane), with carriageways inheriting properties of parent roadways, and lanes in turn inheriting properties of carriageways. Geometry and quality requirements can be associated with each level of representation, and in this broader view it becomes clear that both ±20 cm and ±20 m data have their uses, in their respective applications and cost-benefit domains.

Remote sensing can assist in the survey of centerlines at all levels. Spatial resolution is clearly pivotal, with 30 m imagery suitable for identifying freeway rights of way, and 5 cm aerial photography appropriate for detailed asset inventory. Spectral resolution is an issue as well: high spectral resolution can often offset inadequacies in spatial resolution, particularly with regard to automated extraction. Multispectral Thematic Mapper (TM) imagery from the Landsat7 missions is inexpensive and widely available for the world. To what extent could imagery of this type, appropriately processed, offer centerline surveyors a source of road geometry or other data relevant for infrastructure management?

As with any centerline survey method, the comparative economics of remote sensing depend on the density of roadways and accessibility of the area. The effectiveness of remote sensing further depends on the ability to distinguish between roads and surrounding surface materials. In rural areas where asphalt roads are surrounded by vegetation, the problem is relatively simple, impeded only by foliage and cloud cover. Urban areas present a difficult challenge, however, because

of the abundance of artificial materials such as driveways and roofs that have spectral properties substantially similar to those of roads. Because context has much to do with centerline extraction, the road extraction problem has to be considered as part of the wider issue of classification and mapping of urban materials.

An important element in this research is the development of a Spectral Library of urban material reflectance. In general this provides a reference against which urban materials can be compared and identified. A library can be developed using either a handheld spectrometer in the field, or unambiguous material signatures (i.e. known to be pure or unmixed) from remotely sensed imagery, with appropriate corrections applied in either case. One value of the library is in cataloguing variations in observed signatures in space and time. Clearly the library is most useful at the highest spectral resolution possible because it can be coarsened to match samples of lower resolution data. The discussion below is centered on hyperspectral data and analysis. The Jet Propulsion Laboratory's 224-band Airborne Visible/Infrared Imaging Spectrometer (AVIRIS) has flown a series of annual missions over parts of urban Santa Barbara, producing reliable data in at least three consecutive years. In addition, more than 6,000 additional point spectra have been recorded with a field spectrometer.

This paper focuses on three applications of the spectral library:

(a) The ability to detect roads in hyperspectral imagery, producing centerline maps. This was discussed above.
(b) The ability to sense pavement health. Oxidation, fading and contamination of asphalt affect its appearance over time, and extensive pavement cracking probably affects signatures even at the 4 m pixel level. Remote sensing is unlikely to be as thorough as field survey in evaluating pavement quality, but in terms of cost and turnaround time, there may be significant potential benefits for some applications.
(c) Spectral reduction or tuning. The purpose is to identify wavebands that best discriminate between urban materials, particularly pavement. If those bands are sufficiently limited and consistent, it may be possible to design a lower spectral resolution (i.e. multispectral) sensor, optimized for urban/transportation infrastructure mapping, that could achieve comparable results at a far lower cost.

DATA AND METHODS

The remote sensing and ground reference data were acquired in the urban area of Santa Barbara and Goleta, California. The study area is characterized by a versatile mix of urban land cover types and surface materials including various categories of roofs and different road types and conditions.

Remote Sensing Data

The study used remote sensing data from AVIRIS acquired on the 9th of June, 2000. The data sets were acquired at a spatial resolution of approximately 4 meters (original low altitude AVIRIS resolution ~ 3.6 m), which is similar to current high spatial resolution space-borne sensor systems like IKONOS. They meet the generally proposed spatial resolution standard of less than 5 m for detailed urban area mapping (Welch 1982), and the high spectral resolution lends itself well to comparative land cover mapping. The AVIRIS sensor acquires 224 individual bands with a bandwidth of ~ 10 nm each, covering a spectral range from 350 to 2500 nm (Green et al, 1998). The data were intensively processed by the Jet Propulsion Laboratory (JPL) in Pasadena and the University of California, Santa Barbara (UCSB) for motion compensation and reduction of geometric distortions due to topography. However, the data required further geo-rectification to fit them to current digital databases of the study region. Reflectance retrieval is a mandatory preprocessing step in detailed spectral analysis of remote sensing data, and for comparison with the spectral library. This step reduces atmospheric affects, and calibrates the signal to reflectance of a defined surface feature describing the percentage of incoming radiation reflected by the object. For this study, radiometrically corrected/georectified AVIRIS data were processed to apparent surface reflectance using modified Modtran radiative transfer code (Green et al, 1993; Roberts et al, 1997), adjusted using a ground reflectance target (Clark et al, 1993). Due to atmospheric contamination, the number of AVIRIS bands was reduced to 180, with the bands 1-7, 105-119, 152-169, 221-224 excluded from the analysis.

The study also investigated the capabilities and limitations of current space-borne satellite systems. An additional data set consists of an image mosaic of seven individual multispectral IKONOS scenes (4 m spatial resolution) acquired in April, May and July 2001. The pre-processing of the data included geometric correction and normalization of atmospheric effects, to provide a consistent and calibrated data set covering the entire Santa Barbara South Coast area. Furthermore, multispectral bands of IKONOS data were simulated from the AVIRIS data for a detailed analysis of sensor limitations in terms of spectral resolution. This step used sensor specific spectral functions that are available from the data vendor, and were convolved to AVIRIS wavelengths. In summary, the final remote sensing data set used in the analysis are an AVIRIS scene with 180 bands, an IKONOS scene simulated from AVIRIS, and an IKONOS mosaic of seven individual images covering the whole Santa Barbara South Coast, all in 4 m spatial resolution.

Ground Reference Data

Field spectra were acquired with an Analytical Spectral Devices (ASD) Full Range (FR) spectrometer (Analytical Spectral Devices, Boulder, CO) on loan from the Jet Propulsion Laboratory. The spectrometer samples a spectral range of 350-2500 nm. The instrument uses three detectors spanning the visible and near infrared (VNIR) and short-wave infrared (SWIR1 and SWIR2), with a spectral sampling interval of 1.4 nm for the VNIR detector and 2.0 nm for the SWIR detectors. All spectra used in this study were resampled to a spectral resolution of 2 nm. A fiber optic cable transmits light from the aperture to the spectrometer. Both the bare fiber, with a field of view of 22°, and an 8° field of view foreoptic lens were used to acquire field spectra.

The spectra of characteristic urban surfaces, including built-up materials (e.g. various roof types and road materials) and non-built up surface types (e.g. green vegetation, non-photosynthetic vegetation and bare soil), were measured in the Santa Barbara urban area. Most surface materials were measured *in situ*, although spectra of new roofing materials were also acquired for several roofing types. Spectra of *in situ* materials were acquired from a height of 1 meter using the bare fiber optic cable, with a field of view of 22° (0.39 m at a height of 1 m). Spectra of new roofing materials were acquired from a height of 0.15 meter, using a 8° foreoptic lens (0.04 m at a height of 0.15 m). More than 6000 spectra were measured between May 23 and June 5, 2001. Spectra were acquired in sets of 5 for each field target. Four to six sets of spectra were bracketed by measurements of a Spectralon (Labsphere, North Sutton, NH) reflectance standard. Spectra were inspected for quality, and suspect observations were discarded. Standard spectra were averaged to create a reference spectrum for the bracketed urban surface spectra. Each urban surface spectrum was divided by its appropriate standard spectrum to create a reflectance spectrum. The approximately 6000 reflectance spectra, representing 147 unique surfaces, make up the Santa Barbara urban spectral library. The spectra were used to analyze the spectral properties of urban materials, road conditions and land cover types, for assessment of suitable spectral bands in separating those materials and image preprocessing as wells as training and validation of the image classification.

Analysis methods

The analysis of the spectral library and the remote sensing data has applied several specific methods. The quantitative assessment of spectral discrimination between urban targets and spectral bands that contribute most to their accurate separation was performed using the public domain program "MultiSpec." This program was designed for processing and analyzing high-dimensional and hyperspectral remote sensing data sets (Landgrebe and Biehl 2001). The central spectral separability measure is the Bhattacharyya distance:

$$B = \frac{1}{8}[\mu_1 - \mu_2]^T \left[\frac{\Sigma_1 + \Sigma_2}{2}\right]^{-1} [\mu_1 - \mu_2] + \frac{1}{2} \mathrm{Ln} \frac{\left|\frac{1}{2}[\Sigma_1 + \Sigma_2]\right|}{\sqrt{|\Sigma_1||\Sigma_2|}}$$

where μ_i and $?_i$ are the mean vector and the covariance matrix of class I respectively.The Bhattacharyya distance is a sum where the first part represents the mean difference component and second part the covariance difference component (Jimenez and Landgrebe 1997). In the recent literature, the Bhattacharyya distance has been proposed as useful measure of separability of band prioritization to decrease the dimensionality of hyperspectral data sets, and to select most suitable spectral bands for data analysis (Chang et al. 1999). The advantage of the Bhattacharyya distance is the close relationship to image classification accuracy (Landgrebe 1998) and the large dynamic range of values that allows detailed analysis of high-dimensional data sets as used in this study. A general problem results from the fact that the absolute values are hard to interpret in terms of deciding whether or not two classes can be separated, hence there are no defined thresholds. Quantitative investigations should be based on relative comparison between different classes, targets or classification levels. The remote sensing image analysis applied the public domain program "MultiSpec" for standard Maximum Likelihood classification techniques, and the software system "eCognition" for the exploration and application of object-oriented image classification.

RESULTS

The presentation of results begins with the assessment and analysis of the spectral library, showing representative road conditions and spectral separability of urban surface types on the material scale. Considering that the spectral library provides fairly pure and accurate spectra, interpretation and analysis gives a "generic" view of the related issues with implications for urban area remote sensing, i.e. if specific materials are not spectrally distinct in the library they will not be separable in remote sensing data sets that operate on the scale of land cover types with 4 m spatial resolution. The second part focuses on the remote sensing data analysis of AVIRIS and IKONOS data. It explores the mapping of urban land cover with special focus on different road types. We discuss and assess innovative image analysis approaches using object-oriented techniques as potential avenues for more accurate mapping of roofs versus roads. Based on those results we further investigate the spectral limitations of current sensor systems, and evaluate and discuss the issue of most suitable spectral bands for mapping urban environments.

Analysis of urban spectral library

Figure 1 presents the spectra of typical road and roof materials. They show a general spectral shape of increasing reflectance for longer wavelengths and with a reflectance peak in the SWIR. Concrete and gravel roads have the highest reflectance; parking lots have the lowest over the entire spectral range. The road material spectra contain absorption features in the SWIR that can be related to their mineral components. Red tile roofs and wood shingle roofs show different spectral signatures compared to the other materials. Both roof types show a significant reflectance increase in the NIR and SWIR region. The wood shingle signature contains the ligno-cellulose absorption feature in the SWIR that is common for all non-photosynthetic vegetation surfaces. The gravel roof spectrum has a signature similar to that of the gravel road, with increasing reflectance towards longer wavelength and a dip in NIR reflection. Tar, gray tile and composite shingle materials show the lowest reflectance with small absorption features in the SWIR, and they have a spectral signature similar to that of asphalt roads. The small-scale variations at ~950 nm are an artifact of the field spectrometer and represent the area of transition between the materials used in the sensor. Other sensor induced spectral variations relate to the "noisy" signal in the SWIR II region above 2300 nm. These artifacts are present in all spectra and especially appear in low reflectance targets.

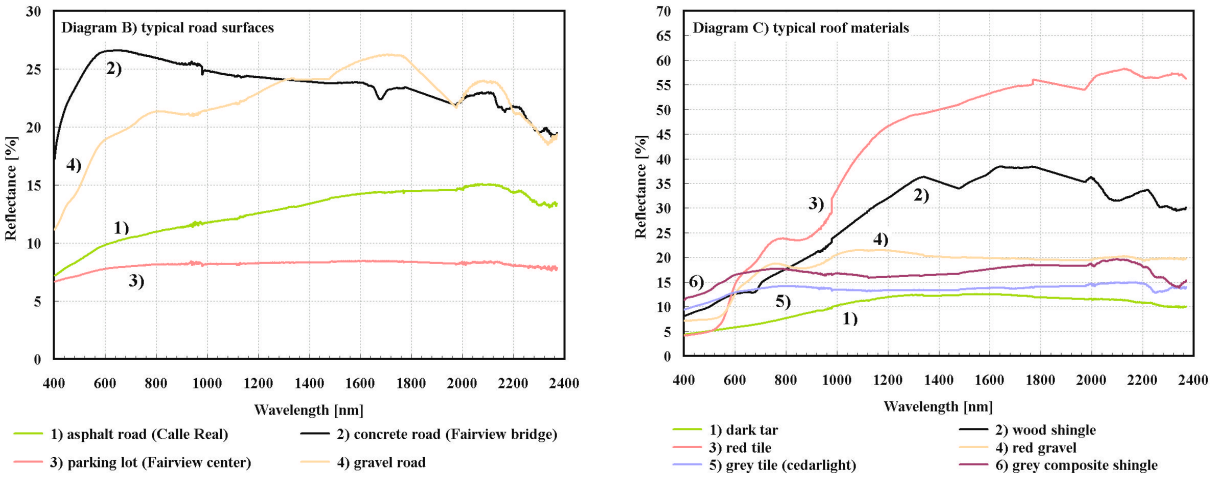

Figure 1: Spectra of typical road and roof materials from the Santa Barbara urban spectral library (the major water vapor absorption bands are interpolated, note the different scales in the y-axis).

Figure 2 represents the spectral variation of transportation surface material conditions. Diagram 2-A shows the change in road with age and use, and its effect on spectral response. New asphalt surfaces have the lowest reflectance with an increasing signal towards 2100 nm. At wavelengths longer than 2100 nm the spectra indicates specific absorption features due to material composition and condition. The older the asphalt, and the poorer the road surface condition (e.g. cracks), the more the reflectance increases in all parts of the spectrum. The difference in reflectance is in the NIR and SWIR I. The comparison of the road spectra also indicates that the depth of the absorption features in the SWIR II is highest for new road surfaces, and decreases with poorer road conditions. These spectral variations represent an interesting spectral contrast that might be used to map road condition using hyperspectral remote sensing systems.

Diagram 2-B presents the variations in spectral response from concrete sidewalk surface due to age or condition. Brand new concrete sidewalk surfaces have the highest reflectance. Aging and poorer condition of the concrete results in decreased reflectance, with the largest reflectance drop in the visible and near-infrared region. The concrete material spectra show absorption features in the SWIR II region. The absorption depth at 2200 nm seems to increase for sidewalks in poorer condition. As noted for asphalt roads, these features should be investigated in more detail as they might be of value in detailed mapping of road condition. Diagram 2-B also shows a spectrum of a sidewalk completely shaded by a tree. The signature resembles the generally low reflectance and spectral features of green vegetation, e.g. the red edge and water absorption bands. The signal results from light transmitted through the foliage cover, and also light reflected downwards from the tree; both impose a vegetation signal on the sidewalk.

These signatures of land cover types and urban materials clearly indicate their spectral separability, at least in terms of visual appearance of their signatures. A further quantitative evaluation of spectral discrimination is provided by the Bhattacharyya distance (B-distance). Figure 3 shows the spectral separability between road materials and roof types. Each individual point represents a B-distance score between an individual roof category, specified on the x-axis, and a road type displayed in a specific color. The continuous line in the graphs show the mean B-distance value representing the

average separability (geometric mean of the B-distance values) between the roof target (x-axis) and the specific road class (color). The spread of those points in terms of the B-distance indicate the spectral complexity in the land cover type. For example, the class "concrete road" seems to have a relatively large range of B-distance values in Figure 3, suggesting a high within-class spectral variation. The smallest separability scores found for each roof target shows the minimum spectral discrimination, and clearly indicates spectral similarities between the specific roof and road materials.

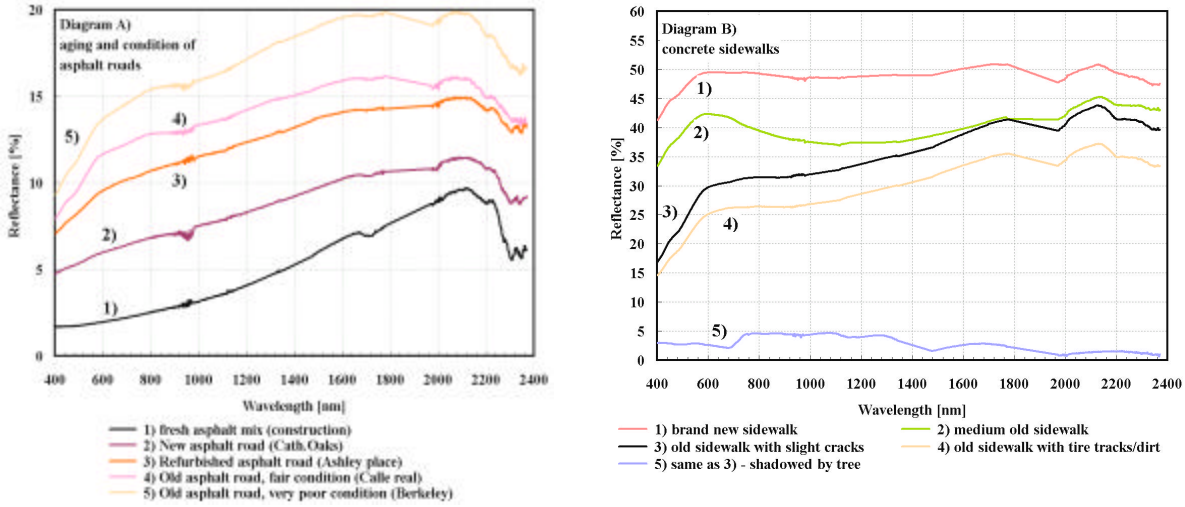

Figure 2: Spectral representation of asphalt and concrete materials conditions (the major water vapor absorption bands are interpolated, note the different scales in the y-axis).

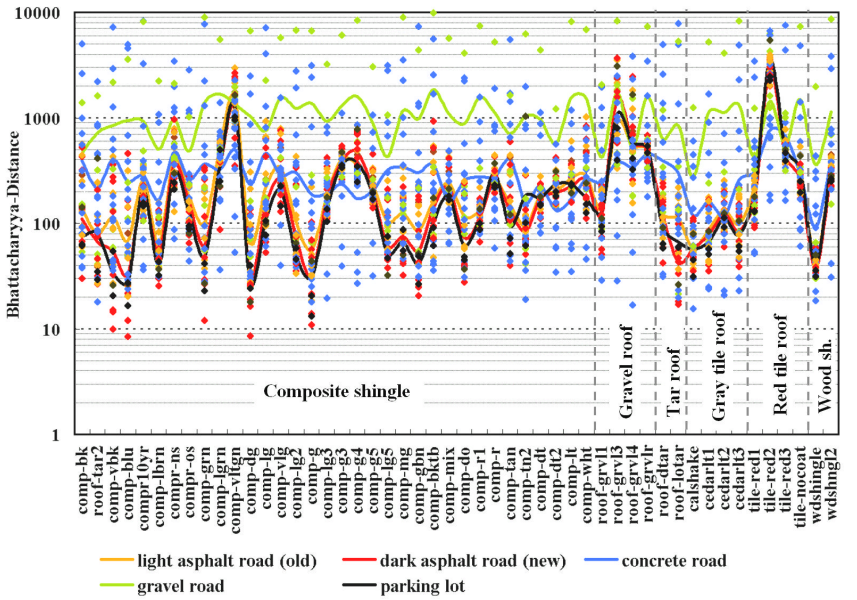

Figure 3: Spectral separability scores (B-distance) for roof materials versus road materials shown as individual points and average measurements shown as lines (geometric mean, note the logarithmic scale of the y-axis).

In terms of the average B-distance values, gravel roads and concrete roofs separate the best for nearly all types of roofs. Parking lots and asphalt roads show a significantly lower average spectral discrimination, with dark asphalt roads (old) and parking lots having the lowest. Especially for composite shingle roofs, tar roofs and gray tile roofs, these surface materials have some significant minimum peaks in average separability below values of 50. The smallest individual values of approximately 10 are for dark asphalt roads versus composite shingle roofs. These values clearly indicate a low separability for those targets, and emphasizes that some roof and road materials are spectrally indistinct, and might not be accurately mapped from remote sensing data. This fact has already been observed in the interpretation of the spectral signatures. The low minimum B-distance values for concrete roads and some roof types are interesting, although concrete roads have a comparatively high average separability. Low individual discrimination is especially obvious for gravel

roofs and gray tile roofs, and again represents the general spectral complexity of urban materials and a high within-class spectral variability (in this case concrete roads) that results in spectral confusion and inaccurate mapping results.

Figure 4 presents the separation of different road types versus asphalt roads. Asphalt roads are most common in the study area, whereas concrete is used for bridges and driveways, and gravel for rural or unpaved roads. Gravel roads have the highest minimum and average B-distance scores and are clearly separated from asphalt roads. Concrete roads show an intermediate average separability but also appear with very low individual values indicating problems in discrimination for specific targets. The least spectral separation is found for parking lots versus asphalt roads as especially shown in the average separability and the minimum individual B-distance scores. Both targets are basically composed of the same material and have similar spectral characteristics, hence are mainly separated by object brightness.

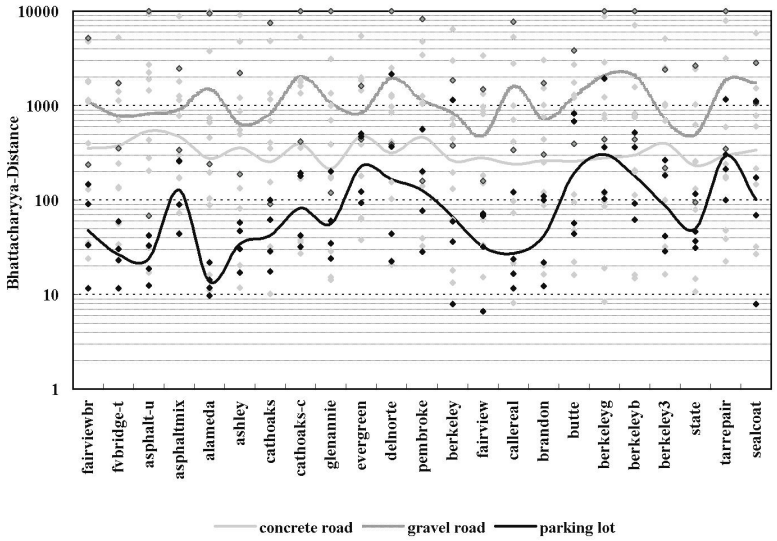

Figure 4: Spectral separability scores (B-distance) for different road surfaces versus asphalt roads shown as individual points and average measurements shown as lines (geometric mean, note the logarithmic scale of the y-axis).

Remote sensing data analysis

The analysis of the spectral library has shown the general spectral similarity between different types of roads and specific roof materials. The classification of the AVIRIS data confirm this result as shown in the error matrix of the AVIRIS land cover classification (Table 1). The table highlights the fairly low producer and user (e.g. Congalton 1991) accuracy for the different road types, with gravel roads showing the highest overall accuracy. Light asphalt roads (representing older asphalt roads) indicate fairly high producer accuracy but are significantly over mapped and confused with other road types and specific roof types (e.g. composite shingle roofs). Dark new asphalt roads are confused with several roof types such as composite shingle roofs and dark tile roofs. Concrete roads are mapped fairly accurately and indicate similarities with light metal roofs and light composite shingle roofs. The results clearly show the problems in mapping roads and road types in an urban environment due to their spectral confusion with specific roof types.

The results shown in Table 1 are based on the analysis of AVIRIS data, hence the most suitable bands from the set of 224 bands representing the full spectral range from 350-2500 nm. Most current high-spatial resolution satellite systems are characterized by a limited spectral resolution. Their spectral bands are broad and cover specific spectral regions, e.g. IKONOS has four multispectral bands representing the visible blue, green, red and near-infrared. It can be assumed that IKONOS has specific limitations in mapping urban areas in terms of its spectral resolution. This issue is discussed in the next section, Sensor Limitations. However, there are innovative image processing techniques that might be able to improve the mapping of roofs versus roads. For example, the object-oriented image analysis approach provides a new and innovative avenue in the analysis of high spatial resolution (2.5 m – 4 m) sensors that represent urban land cover objects such as buildings and roads in a number of adjacent pixels, as shown in the Normalized Difference Vegetation Index (NDVI, Tucker 1979) image of Figure 5. Object oriented image classification is based on image segmentation that focuses the analysis on homogenous image objects rather than on individual independent pixels (Blaschke & Strobl 2001). The image classification can also include spatial and contextual object characteristics as additional levels of information in land cover type separation and mapping the complex urban environment. Figure 5 shows the object length/width ratio, which highlights roads, and provides a unique separation feature to roads.

	Producer Accuracy (%)	Sample	1	2	3	4	5	6	7	8	9	10	11	12	13	14	15	16	17	18	19	20	21	22	23	24	25	26
1: br_comp_sh	**48**	100	48	5	3	7	--	-	-	-	-	1	28	-	-	-	-	-	-	-	-	-	-	-	-	-	-	-
2: dkgr_comp_sh	**50**	100	1	50	16	-	-	-	-	-	-	3	16	-	5	2	-	-	-	-	2	4	-	-	1	-	-	-
3: ltgr_comp_sh	**63**	100	-	15	63	-	9	-	-	6	-	1	4	-	-	1	-	-	-	-	1	-	-	-	-	-	-	-
4: tan_comp_sh	**52**	100	3	-	9	52	-	-	2	5	-	11	12	-	-	2	-	-	-	-	2	-	2	-	-	-	-	-
5: gr_gravel_rf	**95**	100	-	-	3	-	95	-	-	2	-	-	-	-	-	-	-	-	-	-	-	-	-	-	-	-	-	-
6: red_gravel_rf	**65**	100	-	-	-	-	-	65	-	2	-	15	14	-	-	4	-	-	-	-	-	-	-	-	-	-	-	-
7: brwn_metal_rf	**62**	100	1	7	6	-	-	-	62	6	-	2	15	-	-	-	-	-	-	-	1	-	-	-	-	-	-	-
8: lt_gr_metal_rf	**69**	100	-	-	29	-	1	-	-	69	-	1	-	-	-	-	-	-	-	-	-	-	-	-	-	-	-	-
9: ltgr_asphalt_rf	**73**	100	-	-	18	-	3	-	-	5	73	-	-	1	-	-	-	-	-	-	-	-	-	-	-	-	-	-
10: red_tile_rf	**92**	100	-	-	-	-	-	-	-	1	-	92	6	-	1	-	-	-	-	-	-	-	-	-	-	-	-	-
11: grbr_tile_rf	**52**	100	2	8	11	1	-	-	4	5	-	13	52	-	1	-	-	-	-	-	1	1	-	-	1	-	-	-
12: dk_tar_rf	**43**	100	-	-	19	-	1	-	-	14	2	5	11	43	-	1	-	2	-	-	-	-	2	-	-	-	-	-
13: wood_sh_rf	**82**	100	-	-	1	-	-	-	-	2	-	8	4	-	82	3	-	-	-	-	-	-	-	-	-	-	-	-
14: green_veg	**95**	100	-	-	-	-	-	-	-	-	-	-	-	-	-	95	5	-	-	-	-	-	-	-	-	-	-	-
15: non_ph_veg	**100**	100	-	-	-	-	-	-	-	-	-	-	-	-	-	-	100	-	-	-	-	-	-	-	-	-	-	-
16: bare_soil	**81**	100	-	-	-	-	-	-	-	-	-	-	-	-	-	5	13	81	-	-	1	-	-	-	-	-	-	-
17: water	**98**	100	-	-	-	-	-	-	-	1	-	-	1	-	-	-	-	-	98	-	-	-	-	-	-	-	-	-
18: swim_pool	**96**	100	-	-	1	-	-	-	-	1	-	2	-	-	-	-	-	-	-	96	-	-	-	-	-	-	-	-
19: lt_asph_road	**89**	100	-	-	3	-	-	-	-	-	-	-	4	-	-	-	-	-	-	-	89	2	-	-	1	1	-	-
20: dk_asph_road	**55**	100	-	1	10	-	-	2	-	-	-	4	8	-	1	1	-	-	-	-	15	55	-	-	1	2	-	-
21: lt_concr_road	**71**	100	-	-	8	-	-	-	-	11	-	-	-	-	-	-	-	-	-	-	10	-	71	-	-	-	-	-
22: lt_gravel_road	**83**	100	-	-	-	-	-	-	-	15	-	-	-	-	-	-	-	1	-	-	1	-	-	83	-	-	-	-
23: parking_lot	**37**	100	1	1	5	-	-	-	-	2	-	3	5	-	-	4	-	25	-	-	12	3	-	-	37	2	-	-
24: railroad	**90**	100	-	-	3	-	-	-	-	-	-	1	1	-	-	-	-	-	-	-	5	-	-	-	-	90	-	-
25: gr_tennis_crt	**95**	100	-	-	-	-	-	-	-	-	-	4	-	-	-	-	-	-	-	-	-	-	-	-	-	-	95	1
26: red_sport_tar	**76,7**	73	-	-	-	-	-	-	-	-	-	17	-	-	-	-	-	-	-	-	-	-	-	-	-	-	-	56
	TOTAL	2573	56	87	208	60	109	67	68	147	75	183	181	44	90	118	118	109	98	96	140	65	75	83	41	95	95	57
	User Accuracy (%)		**85,7**	**57,5**	**30,3**	**86,7**	**87,2**	**97**	**91,2**	**47**	**97,3**	**50**	**29**	**97,7**	**91**	**80,5**	**85**	**74**	**100**	**100**	**64**	**85**	**95**	**100**	**90**	**95**	**100**	**98**
Overall accuracy: (1892/2573) = 73.5 % **Kappa = 72.5%** **Kappa variance = 0.000082**																												

Table 1: Error matrix of AVIRIS land cover classification highlighting the accuracy and confusion of road types.

The object-oriented image segmentation and classification using the eCognition software was applied to the IKONOS mosaic of seven individual images covering the whole Santa Barbara urban area. The classification in eCognition was implemented as a hierarchical system with Level I classes comprising water, built up, vegetation, and bare land surfaces. The Level I classes were separated using spectral information (nearest neighbor distance), except for bare soil/beach/bare rock areas, which were constrained by a minimum object size to avoid confusion with specific roof types. Another minimum size rule was applied for water bodies, to include another separation criterion to shadows and swimming pools. The Level II built up class (roofs, and transportation areas) were separated using spectral and shape information. Usually road image objects are determined by a linear structure whereas buildings have more compact shapes. We used the length/width ratio of objects to represent this feature in the classification process.

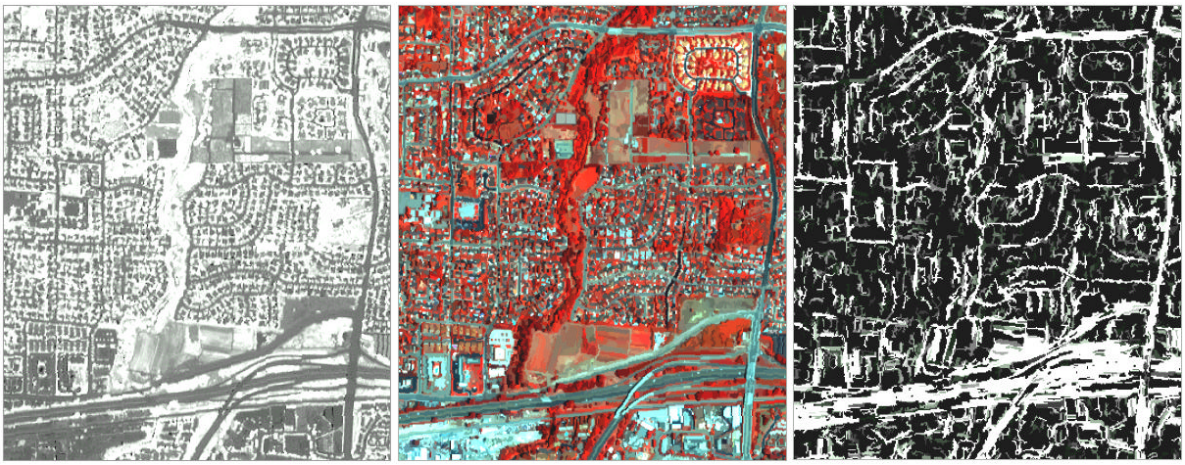

Figure 5: NDVI image subset (left), segmented image derived from IKONOS in channel 4,3,2 color composite (center) and length/width ratio of the segmented image objects.

Figure 6 shows the comparison of the final results of the classification to a false color composite, and digital data layers of buildings and roads. The overall land cover pattern of vegetation, buildings, and roads are well represented in the classified map. The land cover categories appear as homogenous objects due to the object-oriented approach used for classification, providing a sophisticated and accurate representation of the real world structures. The accuracy of road mapping is

for producer and 64% for user accuracy, which is good considering the low spectral resolution of the IKONOS sensor, and shows the usefulness of object-oriented approaches in mapping roads from remote sensing data.

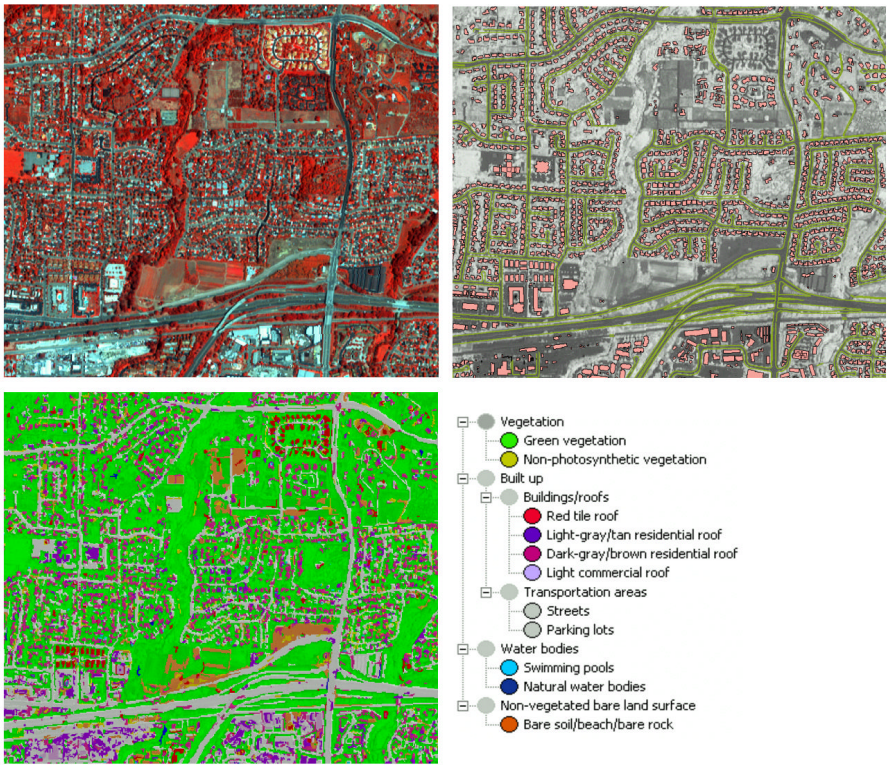

Figure 6: eCognition classification result (bottom) compared to IKONOS false color composite (upper left) and digital data representing house and roads overlaid the NDVI (upper right).

Once the roads or specific road types are classified from remote sensing data, the mapping product might be used to derive road centerlines. This process has to consider the inaccuracies in the mapping process and the spatial resolution of the remote sensing system. Given the mapping result from the AVIRIS data, the process of centerline extraction is presented in Figure 7. Note that Figure 7(c) incorporates results of separate processes of linear filtering (to remove non-linear features such as roofs and other isolated pixels), gap removal, vectorization and smoothing.

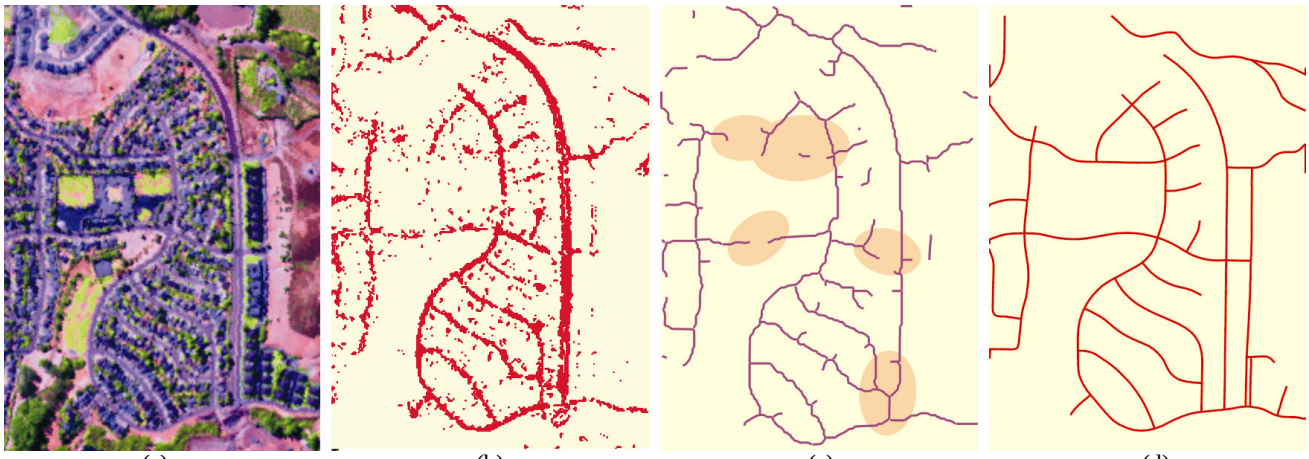

(a) (b) (c) (d)

Figure 7: (a) AVIRIS image, (b) Classification of road surfaces (includes some driveways and roofs), (c) Linear filter applied, gaps removed, and centerlines vectorized and smoothed, (d) Reference centerline map for comparison. Principal areas of disagreement are highlighted in (c); some discrepancies arise because the imagery predates the map. Driveways are easily removed by analysis of connectivity and length.

Sensor limitations and implications for multispectral sensor design

The spectral resolution of current high-spatial resolution space borne remote sensors is significantly lower than the resolution provided by AVIRIS. Also, the spectral sensor characteristics of those earth observation systems were designed for mapping a variety of surfaces, especially for acquisition of natural and quasi-natural environments. Considering the unique spectral characteristics and complexity of urban land cover types, it can be assumed that there are specific limitations in detailed mapping of such an environment. Accordingly, it is important to assess these limitations and to explore most suitable settings of spectral resolution for a multispectral sensor designed as an "urban mapper."

The limitations of IKONOS in mapping the urban environment are shown in Figure 8, which indicates the improvements in classification considering different spectral sensor characteristics. These investigations are based on IKONOS simulated from the AVIRIS data and sensor configurations that have been found most suitable in mapping urban areas (described later in this section). Figure 8 compares classification results of 3 sensor configurations of AVIRIS bands to the simulated IKONOS setting. The first, "Top 5 VIS," assumes 5 narrow bands (10 nm bandwidth) in the visible (VIS) and near infrared (NIR) region instead of 4 broad bands like IKONOS. The second setting assumes the IKONOS bands with two additional most suitable bands in the short-wave infrared, a region not covered with IKONOS. Finally, we consider a spectral configuration that uses the 14 most suitable bands from 224 AVIRIS bands that contribute the most to spectral separability of urban land cover classes (this setting was used to derive the AVIRIS classification result as presented in the previous section). The improvements shown in Figure 8 are obvious for nearly all classes, especially for individual roof and road types. No improvement is found for classes that were already mapped at very high accuracy with IKONOS, such as water, vegetation and swimming pools. The figure shows that IKONOS has limitations in detailed urban mapping due to the broad spectral bands and the fact that it does not cover the short-wave infrared region. The improvements are especially evident for different road types, in particular for asphalt and concrete roads and parking lots. For these targets, user accuracy decreases between 10% and 40% given the most suitable setting of Top 14 bands, representing the severe problems of IKONOS in mapping roads in an urban environment. As expected, the most suitable 14 bands show the highest user accuracy for all classes. The derivation of these bands was based on the B-distance that provides a separability score between each land cover class, and can be used to evaluate the spectral bands that contribute most spectral contrast for the separation of the classes. This information can be aggregated to provide a set of most suitable bands for best average and best minimum separability considering all investigated categories. The top scores for best average over all possible band combinations provide the maximum average B-distance score. Respectively, the set of bands for best minimum separation is based on the best minimum B-distance value over all classes.

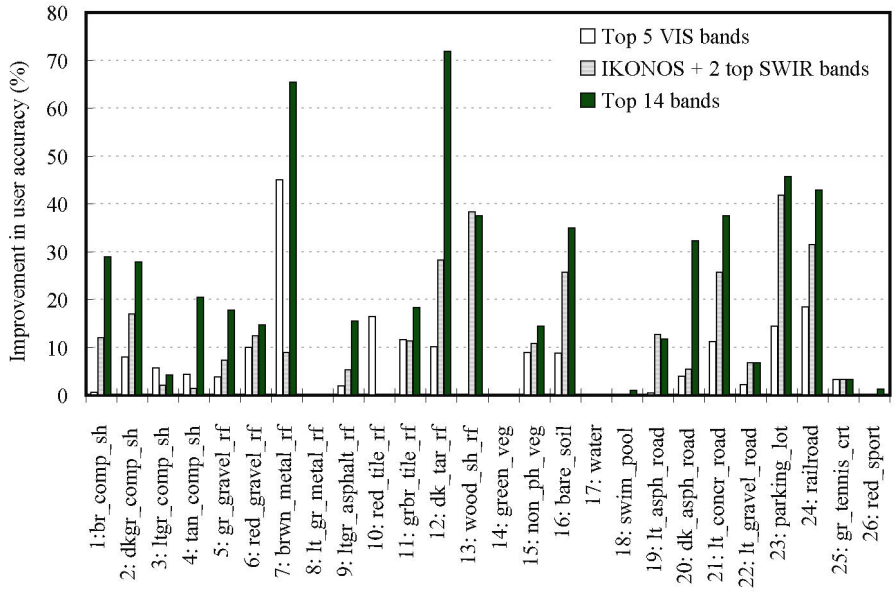

Figure 8: Improvement in classification accuracy for different spectral configurations compared to classification based on IKONOS.

The most suitable bands derived from separability analysis of 108 targets in the spectral library and in separating 26 land cover classes in the AVIRIS data, are shown in Figure 9. The graph presents the frequency of each spectral band's appearance considering the top 20 combinations of 9 bands for best average separability, and of 7 bands for best minimum separability for the spectral library and the AVIRIS data. A band can have a maximum frequency of 40 as it can appear in all of top channel combinations. In Figure 9, a number of bands have a score of 20 as they appear in all of the top 20 combinations for either best spectral library or AVIRIS separability. Some of the top band appearances have a frequency of 1 and mostly appear in a number of adjacent bands (e.g. at 1700 nm) and represent an important "most suitable" spectral region without prioritization of a particular band.

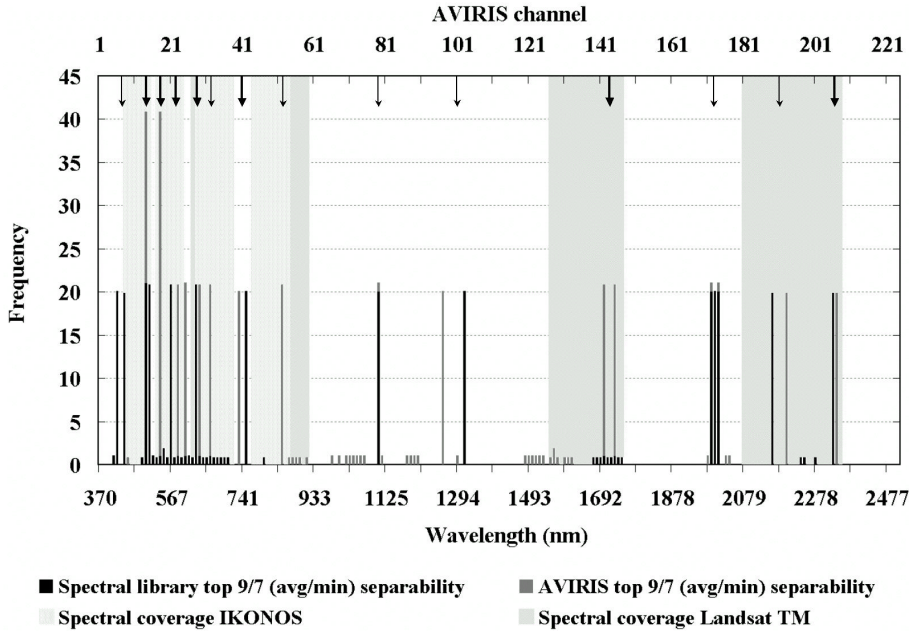

Figure 9: Frequency of appearance of most suitable spectral bands for best average and minimum separability of targets in the spectral library spectral library and the AVIRIS data compared to the spectral coverage of IKONOS and LANDSAT TM satellite sensors.

The most suitable bands appear for nearly all parts of the spectrum with a fair number in the visible region. This supports the previous analysis that narrow bands should be preferred in this spectral region. Additional bands are in the NIR and

short-wave infrared. These bands represent the spectral discrimination in this region that relate to the increase in object brightness towards longer wavelengths as indicated for most urban targets. Furthermore, there are specific absorption features in the short-wave infrared for different urban targets that correspond to the "optimal" bands in Figure 9.

In terms of designing an "urban mapper" sensor, Figure 9 shows evidence of several important bands, that are confirmed from both the analysis of the spectral library and the AVIRIS data. These bands are marked with a bold arrow in Figure 8, and represent five bands in the visible region (Top 5 VIS) and two additional bands in the SWIR. These bands have been used in the investigation presented in Figure 8. Further marked bands (with a normal arrow) are not strongly confirmed from both sources (spectral library and AVIRIS) but can be considered most suitable for mapping the urban environment. Overall there are 14 bands marked in Figure 9 and correspond to the setting of 'Top 14" bands that have been used in the classification of the AVIRIS data, as presented in previous sections.

Figure 9 also provides an assessment between the locations of most suitable bands and the spectral coverage of two commonly used space borne sensor systems, IKONOS and Landsat TM. The comparison shows that most of the suitable bands lie outside or near the boundaries of the spectral range of those sensors. Furthermore the broad band character of the channels does not resolve small-scale spectral absorption features, especially in the visible and SWIR II region, that have been described for several built up and some non-built up cover types. These results again suggest that these sensors have significant limitations for mapping the urban environment considering different roof materials, road surfaces of variable age and quality, parking lots, bare soil and urban vegetation. These results are of course true of the Santa Barbara region, and might be different if other urban centers are considered. However, this study emphasizes that urban areas represent a spectral diversity that far exceeds that of natural systems. The design of related "optimized" multispectral remote sensors has to take these issues into consideration to meet the needs for detailed mapping of urban land cover, road types and road conditions.

CONCLUSIONS

This study focused on 3 issues: (a) extraction of road centerlines, (b) detecting pavement condition, and (c) investigation of the best discriminators of urban land use types. For the purpose of road detection and centerline extraction, analysis of AVIRIS data is somewhat successful, but not perfect, in urban areas. Within-class spectral variability is high, especially on concrete roads. There is spectral confusion between some types of asphalt pavement and roofing materials. It may be possible to improve the success of centerline extraction and recognition using contextual object oriented image classification, based on geometric morphology (e.g. typical curvatures), topology, spatial proximities, and elevation data from sensors such as Lidar. Given the cost of this processing — and the cost of initial image orthorectification to achieve the required standard of positional accuracy — it would appear that hyperspectral remote sensing is better suited to the *detection* of roads in urban areas, while field methods such as GPS are better suited to their geometric delineation.

The hyperspectral approach to automated centerline mapping is likely to be simpler and more successful in rural areas, because pavement signatures are less prone to confusion with those of surrounding materials. Rural areas are not well suited to field-based mapping technologies such as GPS; changes are relatively difficult to monitor, and positional accuracy specifications are usually less stringent; hence a remote sensing solution would be valuable. This research project was not designed to examine rural areas, but this is a potential area of future effort.

This research has achieved mixed results with regard to pavement health. It is certainly possible to map pavement type (e.g. concrete vs asphalt), and this is useful information. It is also possible to determine gross age of pavement. Transportation professionals are usually more interested in pavement *quality* (e.g. rutting, cracking), but these are sub-meter phenomena and are not detectable in hyperspectral imagery of this resolution. Although cracking and patching tend to be spatially concentrated and therefore potentially detectable in 4 m imagery, the research shows that there is too much within-group variability between pavement aggregates to be able to isolate cracked and patched areas with any certainty.

Ultimately the success of remote sensing in transportation will depend largely on economics. The focus on hyperspectral analysis, particularly using AVIRIS (currently an experimental sensor), can be criticized as being overly complex, inaccessible and too expensive for most agencies. With regard to this issue, this research seeks to generalize the problem to the multispectral level, while addressing the science of material discrimination at the more rigorous 224-band hyperspectral level. This research shows that there is a potential future for a multispectral sensor, tuned to urban and pavement mapping, which because of its lower spectral resolution would be affordable and could see widespread application. One potential role of a sensor such as AVIRIS, is in helping design an optimum instrument.

ACKNOWLEDGEMENT

The authors are grateful for the support of the U.S. Department of Transportation, Research and Special Programs Administration, OTA #DTRS-00-T-0002 (NCRST-Infrastructure).

REFERENCES

Blaschke, T. & Strobl, J. 2001. What's wrong with pixels? Some recent developments interfacing remote sensing and GIS *GeoBIT*, 6(6):12-17

Chang, C. I., Du, Q., Sun, T., Althouse, M. L. G. 1999. A joint band prioritization and band decorrelation approach to band selection for hyperspectral image classification, *IEEE Transactions on Geoscience and Remote Sensing*, 37(6): 2631-2641.

Clark, R.N., Swayze, G.A., Heidebrecht, K.B., Goetz, A.F.H., Green, R.O., 1993. Comparison of methods for calibrating AVIRIS data to ground reflectance. Summaries of the 4th Annual Airborne Geosciences Workshop, Vol. 1 AVIRIS (R.O. Green Ed.) JPL Publication 93-26,31-34.

Congalton, R., 1991. A Review of Assessing the Accuracy of Classifications of Remotely Sensed Data, *Remote Sensing of Environment*, 37:35-46

Curtin K.M, Goodchild M.F., Noronha V.T., 2001. Unified Network for Transportation (UNETRANS). Working draft.

Green, R.O., Conel, J.E. and Roberts, D.A., 1993, Estimation of Aerosol Optical Depth, Pressure Elevation, Water Vapor and Calculation of Apparent Surface Reflectance from Radiance Measured by the Airborne Visible-Infrared Imaging Spectrometer (AVIRIS) using MODTRAN2, *SPIE Conf. 1937, Imaging Spectrometry of the Terrestrial Environment*, 2-5.

Green, RO, Eastwood, ML, Sarture, CM, Chrien, TG, et al., 1998. Imaging spectroscopy and the Airborne Visible Infrared Imaging Spectrometer (AVIRIS). *Remote Sensing of Environment* 65(3):227-248

Hepner, G. F., Houshmand, B., Kulikov, I. and Bryant, N. 1998. Investigation of the integration of AVIRIS and IFSAR for urban analysis, *Photogrammetric Engineering and Remote Sensing*, 64(8):813 – 820.

Jimenez, L. and Landgrebe, D.A. 1999. Hyperspectral data analysis and supervised feature reduction via projection pursuit, *IEEE Transactions on Geoscience and Remote Sensing*, 37(6):2653-2667.

Landgrebe D.A., Biehl, L. 2001. An introduction to MultiSpec, URL: *www.ece.purdue.edu/~biehl/MultiSpec/*

Noronha V.T. 2001. Welcome Notes. Centerline Extraction and Maintenance (CLEM2001), Santa Barbara. URL: *www.ncgia.ucsb.edu/ncrst/meetings/clem2001*.

Roberts, D. A., Green, R. O. and Adams J. B. 1997. Temporal and spatial patterns in vegetation and atmospheric properties from AVIRIS, *Remote Sensing of Environment*, 62(3):223-240.

Tucker, C. J. 1979. Red and Photographic Infrared Linear Combinations for Monitoring Vegetation. *Remote Sensing of Environment* 8:127-150.

Welch, R. 1982. Spatial resolution requirements for urban studies. *International Journal of Remote Sensing*, 3(2):139-146.